ACS Sustainable Chemistry & Engineering

pubs.acs.org/journal/ascecg

Research Article

Acidogenic Fermentation of Brewers' Spent Grain Monitored through Two-Dimensional Fluorescence Spectroscopy

Eliana C. Guarda, Eunice Costa, Cátia Gil, Catarina L. Amorim, Claudia F. Galinha,* Anouk F. Duque,* Paula M. L. Castro, and Maria A.M. Reis

Cite This: *ACS Sustainable Chem. Eng.* 2023, 11, 7398−7406

Read Online

ACCESS | Metrics & More | Article Recommendations | Supporting Information

ABSTRACT: Biological systems are commonly controlled and monitored through offline and time-consuming tools, which often impairs an effective and real-time response to counteract system disturbances. The feasibility of using two-dimensional (2D) fluorescence spectroscopy as a non-invasive, non-destructive, and real-time procedure to monitor the acidogenic fermentation of brewer's spent grain (BSG) in a granular sludge reactor was evaluated. For that, the effect of pH fluctuations on the system response was used as a model to ascertain the 2D fluorescence spectroscopy applicability to monitor the process performance, namely, to predict the fermentation products (FP) and the soluble protein (SProt) concentrations in the effluent stream through mathematical analysis. The pH fluctuations over the course of the reactor's operation altered the granules' microbiome composition, leading to different effluent FP profiles. Fluorescence excitation−emission matrices (EEMs) were used with projection to latent structures (PLS) modeling to predict the FP and SProt concentrations in the effluent with average errors below 0.75 and 0.43 g L^{-1}, respectively. Both models were able to capture the tendency of the data even when the accuracy of prediction was not so high. The combined approach of using 2D fluorescence spectroscopy and mathematical analysis seemed promising for real-time monitoring of the acidogenic fermentation of complex substrates.

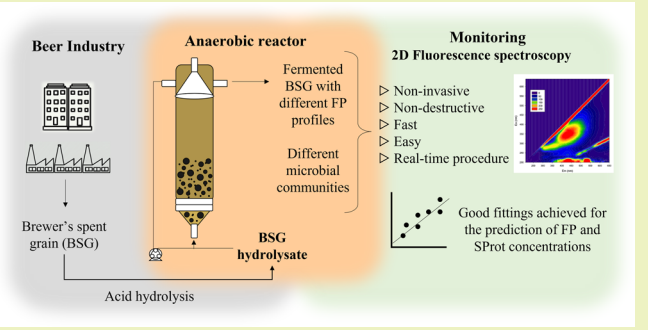

KEYWORDS: *waste valorization, organic acids, 2D fluorescence spectroscopy, microbiome dynamics, fluorescence excitation-emission matrices, multivariate regression*

INTRODUCTION

Nowadays, the performance of biological systems, including control and monitoring, is mostly assessed based on expensive, offline and time-consuming tools such as high-performance liquid chromatography (HPLC) and colorimetric methods, which require extraction steps and the use of analytical reagents.[1,2] Moreover, the sample has to be withdrawn from the system and treated (centrifugation and filtration) for further analysis, increasing the risk of deterioration and/or contamination as well as the time to obtain the analytical result. Often, this does not allow for fast and real-time decisions to monitor and control the process. Some efforts have been conducted to find alternative analytical techniques that allow for in situ and online monitoring and control of the process, like pH, temperature, and dissolved oxygen.[3] They should avoid the use of chemical reagents and waste production, allowing instantaneous data acquisition without time delay and achieving higher efficiency, productivity, and optimization. The development of those innovative analytical tools increases the possibility of an early detection of deviations from the expected process.[3,4]

Fluorescence spectroscopy emerged as a highly promising tool for in situ and online monitoring of biological systems through the use of an optical fiber probe.[5] As the probe can be interfaced in the system, there is no risk of contamination nor sample consumption, making the technique non-invasive and non-destructive.[3,4] Moreover, it is a green environmentally friendly analytical technique as it is chemical- and waste-free. Two-dimensional (2D) fluorescence spectroscopy is performed by simultaneous scanning of several excitation and emission light wavelengths, resulting in excitation−emission matrices (EEMs) where the intensity of emission for each pair of excitation/emission wavelengths is recorded.[2] These spectra enclose information regarding the natural fluorophores present in the system, including several intra- and extra-cellular microbial compounds.[5] Other molecules resulting from the microbial activity (even non-fluorescent) and their interactions are also captured, leading to light interferences. These

Received: January 16, 2023
Revised: April 19, 2023
Published: May 2, 2023

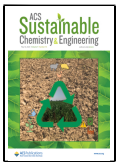

interferences enrich the resulting EEMs by providing an overall fingerprint of the biological system's physiological state.[4] To extract the quantitative information obtained on the fluorescence spectra and solve some limitations (e.g., inner filter effects and quenching), chemometric tools are currently used. These tools have already been successfully applied to monitor fermentation processes, fed-batch cultivations and membrane bioreactors for wastewater treatment.[5−8]

One of the biological systems that can highly benefit from online monitoring is the acidogenic fermentation, which is currently highly dependent on offline and time-consuming analytical tools. Acidogenic fermentation is one step of anaerobic digestion, in which the organic matter is converted into fermentation products (FP) such as volatile fatty acids (VFA), lactate, ethanol, hydrogen, and carbon dioxide.[9] By manipulating the operational parameters, such as pH, different concentrations and profiles of organic acids in the fermented streams can be obtained.[10] Brewer's spent grain (BSG) is the major by-product of breweries, representing about 85% of their total solid residues.[11] BSG is a lignocellulosic residue mainly composed of fibers (hemicellulose and cellulose) (30−50% w/w), proteins (19−30% w/w), and lignin (12−20% w/w). Currently, it is mostly used for animal feed.[11,12] However, the circular economy model targeting for more sustainable process has driven the research of biotechnological processes on the use of BSG to produce added-value products and energy carriers such as biodiesel, bioethanol, biogas, organic acids, polyhydroxyalkanoates (PHAs), enzymes, proteins, sugars, and antioxidants.[10,13−17]

In this work, the feasibility of using 2D fluorescence spectroscopy for the real-time monitoring of BSG acidogenic fermentation was evaluated. The impact of pH changes on acidogenesis was used as a model to ascertain the procedure accuracy. Given the broad potential of 2D fluorescence to monitor biological systems, the fluorescence EEMs obtained along the operation were used to predict the fermentation products (FP) and soluble protein (SProt) concentrations through principal component analysis (PCA) and projection to latent structures (PLS) models. This study aims at demonstrating, for the first time, the possibility of applying 2D fluorescence spectroscopy for the real-time monitoring of a biological system through the correlation between EEMs and the performance parameters.

MATERIALS AND METHODS

Feedstock. Raw BSG supplied by an industrial Portuguese brewery (Super Bock Bebidas S.A., Matosinhos, Portugal) was dried at 70 °C and ground in a hammermill. Dried BSG powder was hydrolyzed as described by Guarda et al.[15] but with some changes. More information related to the pretreatment can be found in the Supporting Information. The BSG hydrolysate obtained had a total chemical oxygen demand (COD) of ca. 62 g COD L^{-1}, being mainly composed of sugars (glucose, xylose, and arabinose) and proteins (data not shown).

Experimental Set-up. An upflow anaerobic sludge blanket (UASB) reactor with a working volume of 1.73 L was inoculated with 520 mL of anaerobic granules from a full-scale anaerobic expanded granular sludge bed reactor (Super Bock Bebidas S.A., Matosinhos, Portugal) and operated with an upflow velocity of 1.4 ± 0.2 m h^{-1}. The reactor was continuously operated at an hydraulic retention time (HRT) of 1 day and at 30.0 ± 0.1 °C using a thermal bath. The OLR was set to 5 g COD L^{-1} day^{-1} during the acclimatization period, including the reactor's start-up. After the acclimatization period, the OLR was increased to 10 g COD L^{-1} day^{-1} and kept constant during the remaining operation time. The pH was continuously monitored and controlled at 4.5 (Stages 2 and 4) or 3.9 (Stage 3) by the automatic addition of 1 M NaOH and 1 M HCl solutions. No extra nutrients were added to the feeding solution due to the high protein content of the BSG hydrolysate, which can be used for the culture metabolism. Reactor and feed samples were taken twice a week for further analysis. More details about the UASB reactor design are found in the Supporting Information.

Analytical Methods. The COD concentration was assessed by a colorimetric method using LCK 914 Hach Lange kits (Hach Lange, Germany). Total and volatile suspended solids (TSS and VSS, respectively) were determined according to the standard methods.[18] The FP and sugar concentrations were determined as previously described by Duque et al.[19] The protein content was measured using the colorimetric method described by Lowry et al.[20] Ammonium (NH_4^+) and phosphate (PO_4^{3-}) contents were determined by colorimetry in a flow-segmented analyzer.[21] A detailed explanation of the methods is given in the Supporting Information.

Microbiome of the Granules. Biomass samples were collected from the reactor and aseptically crushed. The resulting biomass suspension was used for extracting the genomic DNA using a UltraClean Microbial DNA Isolation Kit (Qiagen, Germany). The extracted DNA was used for next-generation sequencing analysis performed at GATC-Eurofins (Konstanz, Germany). Paired-end sequencing based on the 16S rRNA phylogenetic gene was conducted (Illumina MiSeq platform) using the primer sets 357F − TACGGGAGGCAGCAG and 800R − CCAGGGTATCTAATCC, which cover the V3−V4 hypervariable region. The microbiome analysis was performed according to Paulo et al.[22]

2D Fluorescence Spectroscopy. UASB samples—feed and effluent—were assessed by 2D fluorescence spectroscopy using an optical-fiber probe immersed directly in the samples under continuous stirring. Fluorescence spectra were acquired in duplicate with a fluorescence spectrophotometer (Varian Cary Eclipse) every time that a sample was taken from the reactor to be analyzed using the conventional analytical methods. More information about the acquisition of the fluorescence spectra can be found in the Supporting Information.

Data Analysis through Principal Component Analysis. Different datasets were analyzed through PCA: (1) the analytical data (physicochemical composition) obtained from the UASB performance effluent and feed samples and (2) the microbiome dataset. The PCA was performed for different datasets separately and implemented with the PARAFAC algorithm from the n-way toolbox in GNU Octave (version 5.1.0).[23,24] Additionally, the PCA was also used to compress the high amount of information contained in the fluorescence EEMs resulting from 2D fluorescence analysis: (1) using all fluorescence EEMs and (2) using the same fluorescence EEMs acquired for the samples used in the microbiome analysis. More information about the PCA analysis are found in the Supporting Information.

Development of Mathematical Models through Projection to Latent Structures. Mathematical models were developed to follow the performance of the reactor, namely, to predict the concentrations of the FP and SProt (in g L^{-1}) in the effluent based on fluorescence data. The mathematical models were obtained by PLS modeling using the PCs obtained from fluorescence EEMs and the pH of the operation as input parameters. More details about the data used and the development of the models can be found in the Supporting Information. The models were selected based on the root mean square error of cross-validation (RMSECV) and were assessed by the root mean square of prediction (RMSEP, calculated for the validation dataset), the root mean square of calibration (RMSEC, calculated for the calibration dataset), the coefficients of determination (R^2), and the slopes between the prediction and experimental data for both training and validation sets. PLS regression was implemented using the npls algorithm from the n-way toolbox in GNU Octave.[24]

RESULTS AND DISCUSSION

An UASB reactor was operated in a continuous mode for more than 300 days using BSG hydrolysate as feedstock. The reactor

https://doi.org/10.1021/acssuschemeng.3c00316
ACS Sustainable Chem. Eng. 2023, 11, 7398−7406

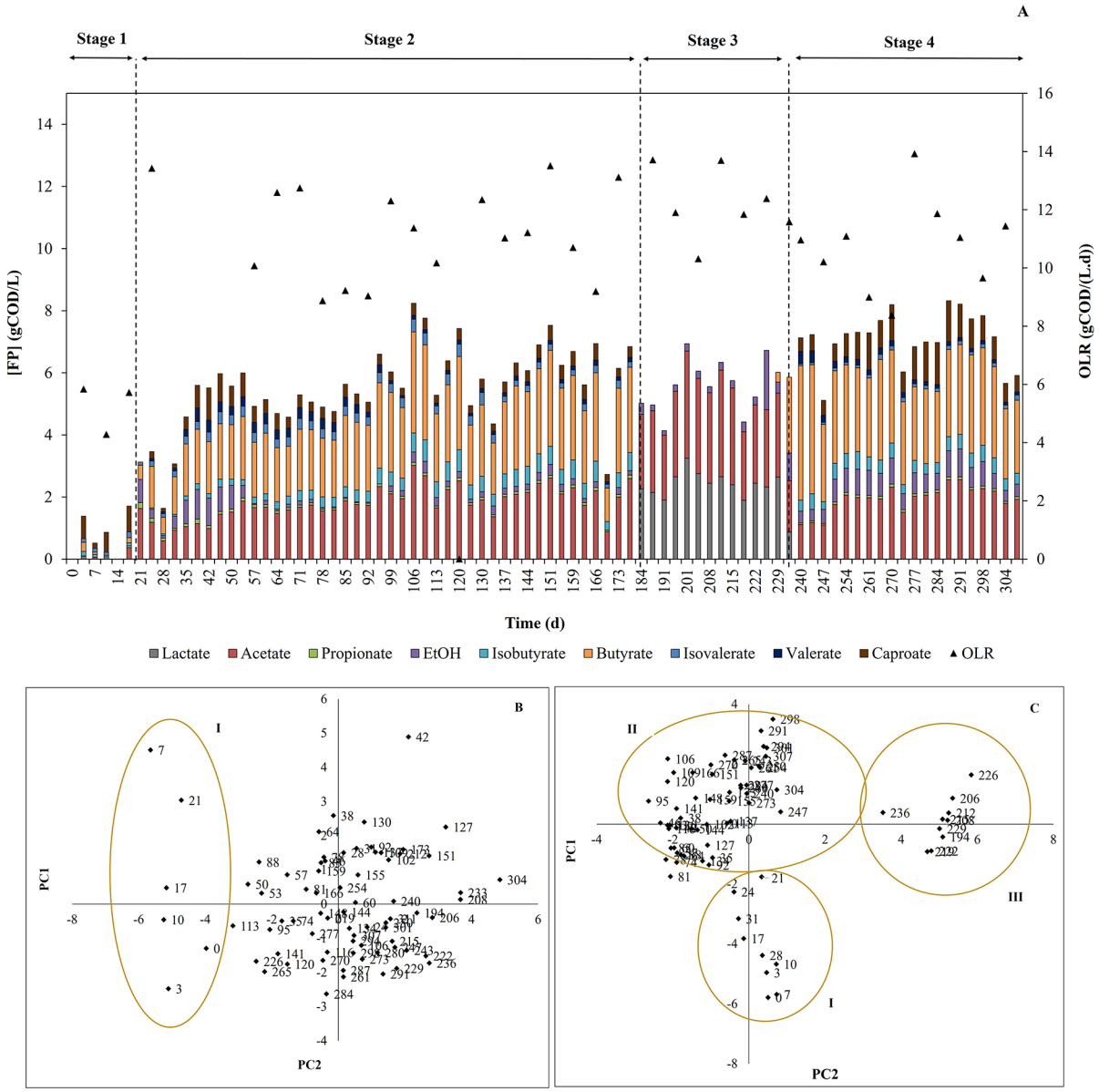

Figure 1. Profiles of FP in the effluent streams and the applied OLR (black triangles) during the four stages of UASB operation using BSG hydrolysate as feedstock (A); scores for PC1 and PC2 from PCA applied to the feed (B) and effluent (C) samples from the UASB reactor throughout the operation. The reactor operational days are presented by the diamonds with numbers while the yellow circles represent the identified clusters (I, II, and III). PC1 and PC2 of maximum variations accounted for 37.3 and 56.2% of the total variation, respectively, for the feed samples and 31.2 and 56.0%, respectively, for the effluent samples.

was operated at different pH and data concerning the fermentation process, and the sludge microbiome dynamics was collected and correlated with the information captured by 2D fluorescence spectroscopy to develop the models.

Reactor Performance. Throughout the UASB operation, the data regarding the different FP profiles achieved from the dynamic change in pH was collected, assuming four different stages. Stage 1 corresponds to the acclimatization period, including the reactor's startup, where the pH was first set at 4.5 to inhibit methanogenic bacteria activity, and the OLR was set at 5 g COD L^{-1} day^{-1} (days 0−17). On day 18, the OLR was increased to 10 g COD L^{-1} day^{-1} and kept constant until the end of operation (Figure 1A). In Stage 2, the reactor's pH was kept at 4.5 (days 18−177), whereas in Stage 3, the pH was decreased to 3.9 (days 178−229) to maintain methanogenic activity inhibition. Last, in Stage 4, the pH was re-established to 4.5 (days 230−307). The overall UASB performance is shown in Figure 1A with more information in the Supporting Information (Table S1). Throughout the operation, the effluent was composed of lactate (HLac), acetate (HAc), propionate (HPr), isobutyrate (HIsoBut), butyrate (HBut), isovalerate (HIsoVal), valerate (HVal), caproate (HCap), and ethanol (EtOH) (Figure 1A and Table S1). All these compounds were previously reported as FP from BSG acidogenesis.[15,16,25,26] The analytical data collected from the feed and effluent samples was analyzed through PCA. Similarities and differences within the feed and effluent samples, individually throughout the operation conditions, were assessed through the scores of the two first principal components (PCs) of the PCA applied to each analytical dataset (Figures 1B and 1C for feed and effluent, respectively).

https://doi.org/10.1021/acssuschemeng.3c00316
ACS Sustainable Chem. Eng. 2023, 11, 7398−7406

The PCA plots from the feed and effluent showed one and three clusters, respectively (Figure 1B,C). In both plots, cluster I mostly contains samples from Stage 1, which grouped more closely and corresponds to an initial system instability related to the reactor startup, where the feed concentration changed according to the OLR increase previously described (days 0−17 of operation). During the remaining reactor operation (days 24 to 307), the PCA of the feed samples did not capture significant differences as no changes on the OLR were performed (Figure 1B). Still, some variability can be observed due to differences in feed pretreatment, preparation, and storage and from the fact that it is a real waste that could slightly change in composition over time. However, the PCA plot of the effluent was able to capture two more clusters (II and III). Cluster II gathered samples from Stage 2 (days 31 to 178) and confirmed the stability of the system as the points representing the operational days were closed to each other and near to the intersection (0,0) (Figure 1C). During Stage 2, the FP profile revealed that the effluent was highly rich in HAc and HBut but also contained small amounts of the other FPs (Figure 1A and Table S1). The cluster III observed in the PCA plot of the effluent samples reflected the change of pH to 3.9 on Stage 3, where the FP profile drastically shifted, with HLac and HAc being the main FP produced (Figure 1A and Table S1). HLac production is usually associated to operation at low pH or to process disturbances.[25,27] The pH increase to 4.5 on Stage 4 shifted the effluent FP profile, which became very similar to the one in Stage 2 as HLac was no longer detected, while HAc and HBut were highly abundant in the FP profile together with small amounts of the other FPs (Figure 1A and Table S1). The effluent PCA plot showed that the samples from Stage 4 grouped together with the ones in Stage 2, forming cluster II and showing the influence of pH on the process performance (Figure 1C). Thus, the effluent PCA plot clearly showed the similar behavior of the system and the resulting FP profiles of Stages 2 and 4, whose samples clustered together and were distant to the ones of Stages 1 and 3. Although some random variability is present in the feed composition, being the highest variance associated with different feed concentration, the changes in effluent FP composition were due to the pH changes applied. The results demonstrated the possibility of manipulating acidogenic fermentation using BSG hydrolysate through imposed pH changes. The return to pH 4.5 resulted in a re-establishment of the FP profile, showing the system's robustness, which had a quick and efficient response to the dynamic pH change as previously observed in other studies.[26] Such conclusions can be confirmed by PCA, which clearly showed the similarities and differences between stages, regardless of the variability within samples (resulting from the dynamic of the system both on the feed characteristics and effluent products).

Granular Sludge Microbiome. *Bacterial Community Dynamics.* Over operation, the effect of pH changes on the granule's microbiome was assessed. The inoculum had a high prevalence of classes such as *Deltaproteobacteria*, *Nitrospira*, and *Bacteriodia*, with *Syntrophaceae*, *Syntrophobacteraceae*, *Syntrophorhabdaceae*, *Prolixibacteraceae*, *Nitrospiraceae*, and *Geobacteraceae* as the most abundant families (Figure S1). After the acclimatization period, the pH of the reactor was set at 4.5 (Stage 2), which gradually altered the microbiome. Bacteria belonging to the *Coriobacteriia*, *Bacteroidia*, and *Clostridia* classes became predominant within the biomass, and *Atopobiaceae*, *Clostridiaceae*, *Prevotellaceae*, and *Ruminococcaceae* became the major represented families (Figure S1). With the decrease of the pH to 3.9 on Stage 3, a pronounced change in the microbiome taxonomic composition was observed. *Lactobacillaceae*, from the *Bacili* class, became the most prominent family, achieving a relative abundance of ca. 81.75% by the end of this stage (Figure S1). The re-establishment of the reactor's pH to 4.5, on Stage 4, led to a new shift in the granules' microbiota, and by the end of this stage, the microbiome composition was very similar to that observed at the end of Stage 2 (Figure S1). By the end of both stages, members belonging to the *Ruminococcaceae*, *Prevotellaceae*, and *Atopobiaceae* families were within the most abundant taxa, together representing more than 63% of the total microbial community. Though the alterations on the pH led to changes in the microbiome composition, on Stage 4, after re-establishing the pH to that of Stage 2, the microbiome taxonomic composition was also re-established.

The PCA plot (Figure 2) reveals that the microbiome composition on Stage 1 (day 0) was markedly different from the

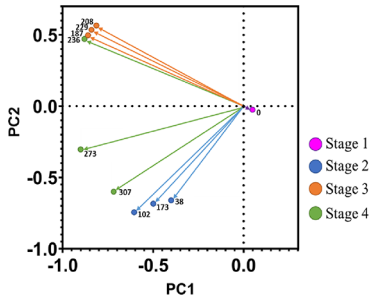

Figure 2. PCA plot of the 16S rRNA gene sequencing data over the different operational stages. PC1 and PC2 of maximum variations accounted for 79.0 and 94.3% of the total variation, respectively.

one in the following stages. This is probably related to the adaptation of the granules' microbiome to the new external environment during the first 38 days of operation, showing that the imposed operating conditions promoted the evolution of the microbial population within the reactor.[25] Furthermore, in the PCA plot, the samples clustered into two major groups: one formed by samples of Stage 3 and the first day of Stage 4 and the other cluster gathering samples from Stage 2 and the remaining samples of Stage 4 (Figure 2). This suggests that the applied pH played an important role in shaping the composition of the granule's microbiome.

Core Microbiome. To evaluate the distribution of taxa among the different stages, a Venn diagram was constructed (Figure S2A). For this analysis, only samples collected from day 102 (Stage 2) onwards were included after achieving process stability. Although a dynamic microbiome was present, a core microbiome composed by 18 different taxa was identified. Nevertheless, a more detailed analysis revealed that from the 18 taxa observed, only 6 were present in all selected sampling days of the reactor's operation. This core of persistence was composed by bacterial species from the *Actinobacteria* (*Bifidobacterium* sp.), *Firmicutes* (*Sporolactobacillus* sp., *Lactobacillus* sp., *Clostridium* sp., and *Clostridium luticellarii*), and *Proteobacteria* (*Acetobacter* sp.) phyla (Figure S2B). The abundance of the core persistent bacteria within the microbiome was variable over time. Except for *Lactobacillus* sp., whose relative abundance in the overall microbiome could reach values of ca. 85% (day 208, Stage 3), the remaining species within the core present low but quite stable relative abundances (up to 8%). Thus, while the applied pH altered the main microbiome

https://doi.org/10.1021/acssuschemeng.3c00316
ACS Sustainable Chem. Eng. 2023, 11, 7398−7406

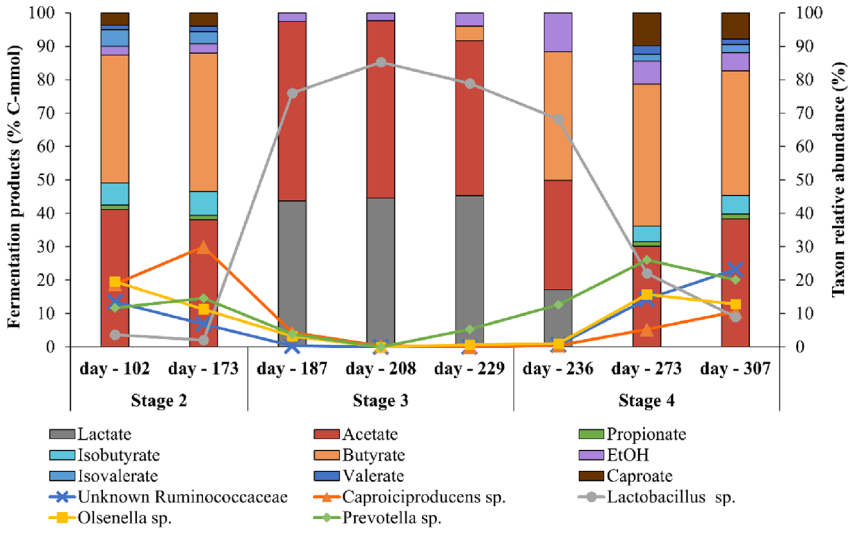

Figure 3. FP production dynamics versus the top 5 most abundant bacterial taxa in each day. The relative abundancies of the FP are shown in bar plots, and the ones of the bacterial communities in linear functions.

composition, there is still a small portion of the population (core microbiome) whose presence is independent of the pH conditions applied. Although present in low numbers within the overall community, these taxa are probably key players, indispensable to maintain the process ecological stability similarly to that reported in the literature.[28] In fact, taxa belonging to the *Firmicutes* and *Proteobacteria* phyla are reported to have more persistent taxa than the other phyla as well as an unexplained stability under anaerobic conditions.[29,30]

Linkage between the Most Abundant Taxa and the Effluent FP Profile. To understand the relationship between the microbiome present in the UASB reactor and the FP produced, the temporal trend of the five most abundant taxa was related with the main FP obtained on each sampling day (Figure 3).

By the end of Stage 2, there was a prevalence of HAc and HBut, which was accompanied by the predominance of bacteria belonging to the *Caproiciproducens* genus in the microbiome with a relative abundance of ca. 30%. Bacteria from the *Olsenella* and *Prevotella* genera were also present although at relative abundances of ca. 15%. The previous referred genera are the ones mainly responsible for the high relative abundances of the *Ruminococcaceae*, *Prevotellaceae*, and *Atopobiaceae* families by the end of Stage 2. The *Olsenella* genera, through fermentation processes and using glucose as a substrate, can produce HAc, EtOH, and HLac.[31,32] The genus *Caproiciproducens* is well known for its ability to produce HAc, HBut, H_2, and HCap, and the *Prevotella* genus is able to perform homoacetic fermentation.[32−34] In addition, the preferred metabolic pathways used by these microorganisms, the butyrate−acetate pathway, and homoacetic fermentation also contribute to the production of HAc and HBut.[35,36] The decrease of pH to 3.9 on Stage 3 altered the microbiome composition as well as the profile of the FP produced. By the end of this stage, the *Lactobacillus* genus prevailed in the biomass, representing about 80% of the overall microbiome, and concomitantly, the highest production of HLac was observed (Figure 3). In fact, on day 229, HLac (ca. 45% Cmmol) and HAc (ca. 46% Cmmol) were the most abundant organic acids in the reactor effluent stream. A reduction of the relative abundance of the remaining top 5 bacteria in the microbiome was observed, such as bacteria from *Ruminococcaceae* family no longer being detected. The changes in pH lead to the activation and deactivation of certain metabolic pathways, thus influencing the dynamics of microbial communities and, consequently, the FP production.[26] In addition, the genus *Lactobacillus* often prefers acidic environments to proliferate, and under conditions of anaerobiosis, bacteria from this genus are able to convert sugars into HLac, which explains the prevalence of such FP during Stage 3.[26,32,37] Plus, members of this genus can carry out homoacetic fermentation, thus explaining the HAc production.[32,33] With the re-establishment of the system pH to 4.5 (Stage 4), the FP profile obtained was like that of Stage 2. A restructuration of the microbiome also happened with the five most abundant taxa resuming their presence in the microbiome, although the relative abundance of each taxon was slightly different from that observed in Stage 2. This result suggests the existence of functional redundancy in the sludge microbiome, which allowed the coexistence of taxonomically distinct microorganisms that can conduct the same metabolic functions. Overall, the microbiome within the granules showed to be highly redundant in its composition, having a high overlap of functions among different species but also quite resilient, with some taxa being able to thrive in the biomass after a process perturbation.

2D Fluorescence for Monitoring the Reactor Performance. 2D fluorescence spectroscopy was assessed to hypothesize the monitoring of acidogenic fermentation, namely, the FP and SProt concentrations at the reactor effluent. For that, the samples collected from the reactor for offline physicochemical reference analysis were also analyzed by 2D fluorescence spectroscopy. Different regions can be observed in a fluorescence spectrum regarding the presence of specific compounds (Figure S3). Some observations related to the complexity of the medium can be captured, resulting in overlays of the fluorescence of different compounds, or maybe due to other compounds in the sample interacting with the fluorophores.[1,4,38] At different days of operation, it is possible to see differences between the fluorescence spectra, showing that fluorescence spectroscopy is sensitive to system variations over time (Figure S3). However, such variations are not clearly correlated with specific performance parameters. Thus, to extract meaningful information, a mathematical approach such

https://doi.org/10.1021/acssuschemeng.3c00316
ACS Sustainable Chem. Eng. 2023, 11, 7398−7406

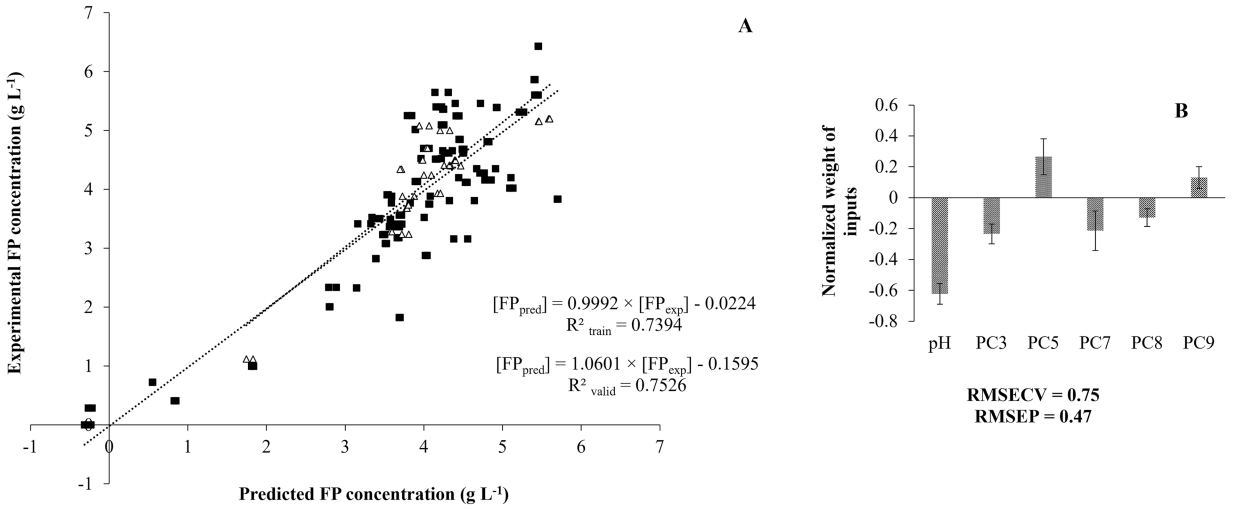

Figure 4. Prediction model (A) and normalized regression coefficients (B) for the FP concentration using the PCs of the effluent samples and the pH. Training values (n = 118, black squares) and validation values (n = 36, white triangles) are presented as FP concentrations (g L^{-1}). PC3, PC5, PC7, PC8, and PC9 are the PCs from the effluent spectra. RMSECV and RMSEP are respectively the root mean square errors of cross-validation and prediction.

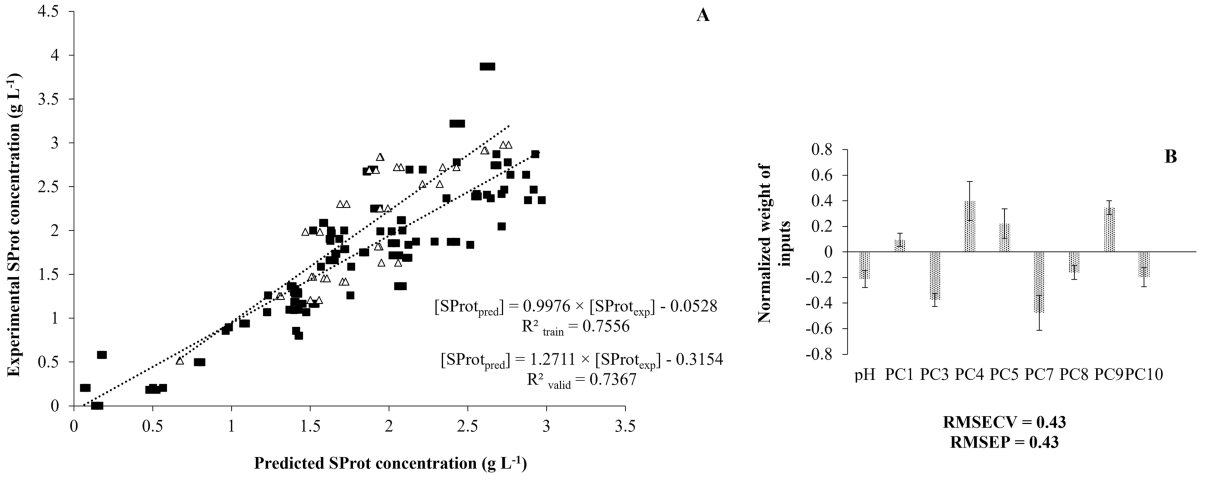

Figure 5. Prediction model (A) and normalized regression coefficients (B) for SProt concentration using the PCs from the effluent samples. Training values (n = 118, black squares) and validation values (n = 38, white triangles) are presented as SProt concentrations (g L^{-1}). PC1, PC3, PC4, PC5, PC7, PC8, PC9, and PC10 are the PCs from the effluent spectra. RMSECV and RMSEP are respectively the root mean square errors of cross-validation and prediction.

as PCA was required. A PCA performed using only the fluorescence EEMs from the same days collected for microbiome analysis can be compared with the PCA from the analytical and microbiome data (Figure S4 and Figures 1C and 2, respectively). All PCAs from the fluorescence, microbiome, and analytical data showed the shifts within the stages, with samples from Stages 2 and 4 clustering more closely (Figure S4 and Figures 1C and 2, respectively). For all datasets, day 236 on Stage 4 is closer to samples from the previous stage (Stage 3), and in fact, the presence of HLac on day 236 shows that the FP profile is changing and becoming similar to those of Stages 2 and 4, but it still has some similarities with Stage 3 (Figure 1C). This shows that although the microbiome started out being selected due to the new imposed conditions, the sample was still more similar to the ones from the previous condition. These results confirmed the ability of 2D fluorescence to capture complex information in the biological system, which seems to be influenced by both the media composition and microbial composition/activity.

To achieve a good correlation and to use fluorescence EEMs as an online monitoring tool, PCA was used to reduce the size of the fluorescence data collected from the effluent prior to establishing correlations with two performance parameters. PLS regression was used to assess the complex correlations between the PCs resulting from fluorescence spectra acquired for the effluent samples and their FP and SProt concentrations determined by conventional analytical measurements. The model for the FP concentration was initially developed using as inputs the 10 PCs resulting from the fluorescence EEMs and the applied operation pH (measured for each sample). After the mathematical selection of inputs, non-useful inputs were eliminated, resulting in better model performance. The results from the optimized PLS model achieved for the prediction of the FP concentration regarding training and validation data are shown in Figure 4. In Figure 4A, the model prediction of the FP

https://doi.org/10.1021/acssuschemeng.3c00316
ACS Sustainable Chem. Eng. 2023, 11, 7398−7406

concentration (x axis) plotted against the experimental values (y axis) reveals a good fitting of the model as the obtained slopes are near 1, meaning that a similar trend between the experimental and predicted values was achieved.

The model achieved for the FP prediction requires five PCs of the 10 initial inputs and the reactor's pH. As shown in Figure 4A, the training and validation R^2, although not very high, were very close to each other (0.74 and 0.75, respectively), showing a good fitting and consistency in the prediction for the validation dataset. Furthermore, the model captured 74.0% of variance and resulted in a RMSEC of 0.72 g L^{-1}, a RMSECV of 0.75 g L^{-1}, and a RMSEP of 0.47 g L^{-1} (Figure 4B). The RMSEP was lower due to the selected dataset for calibration; however, the RMSEC is not substantially different from the RMSECV, showing the robustness of the model. The model results show that the inclusion of the pH data was important to achieve a good prediction of the model as its regression coefficient was higher (meaning higher weight in FP prediction) than the other four PCs from the EEMs matrices, greatly contributing for the improvement of the model (Figure 4B). By plotting the FP concentration (y axis in g L^{-1}) through the time of operation (x axis in days), it is possible to observe that the model captures well the tendency of the experimental data, although it did not predict so well some points where the concentration suddenly changed (days 106, 170, and 180) (Figure S5A in the Supporting Information). However, for those points, the model followed the tendency of decreasing or increasing the FP concentrations, although with higher errors.

For the prediction of the SProt concentration, a similar approach was used to develop the PLS model as shown in Figure 5.

The model achieved after input selection requires 8 PCs from the 10 initial inputs from the fluorescence data and the pH. Training and validation R^2 were 0.76 and 0.74, respectively, the RMSEC was 0.40 g L^{-1}, and the RMSECV and RMSEP were the same (0.43 g L^{-1}), proving the robustness of the model (Figure 5). In Figure 5B, where the normalized regression coefficients are represented, it is shown that the applied pH had again a great contribution for the model as in the model for the FP concentration prediction. However, in this case, the model greatly depends on several PCs obtained from fluorescence EEMs: PC3, PC4, PC7, and PC9, which have the greatest regression coefficients (Figure 5B). Despite the natural fluorescence of proteins, the modeling results show that the prediction of SProt concentrations depends on several regions of the fluorescence spectra, which highlights the complexity of the information contained in the fluorescence spectra and the need to use advanced mathematical tools. By plotting the SProt concentration (y axis in g L^{-1}) through the operation time (x axis in days) (Figure S5B), it is possible to see that similar results to the model of FP prediction were attained. Even when the models cannot predict so well the drastic and sudden variations in concentrations, they are able to follow the tendency of those points. Although PCA and PLS aim to extract the complex information contained in the fluorescence spectra and correlate it with quantitative parameters, the differences in the media and applied pH impact the microbiome and, consequently, the reactor performance and effluent composition. As such, it is difficult to establish correlations between the fluorescence spectra and the quantitative parameters due to changes on the light interferences. Additionally, the accuracy of the methods developed for the prediction of FP and SProt concentrations depend on the quality of the spectra acquired as well as on the quality of the data used for calibration. As the calibration of the PLS models requires the use of analytical values of FP and SProt, the experimental errors of these parameters are also included and relevant when assessing the quality of the models achieved. For instance, the quantification of the SProt was performed using the colorimetric Lowry method, which had an average error of calibration of 5% (in a range of 5 to 100 mg L^{-1}) and 3% average error for duplicates. The FP concentrations were quantified through HPLC (nine different compounds were measured and summed) with an average error of 6.2% for duplicates. Therefore, the accuracy of the predictions by fluorescence is not similar to the standard analytical methods. However, the use of 2D fluorescence is particularly useful as it allows continuous online assessment (each spectra takes approx. 5 min), providing an overview of the tendency of the SProt and FP concentrations.

CONCLUSIONS

Acidogenic fermentation using BSG hydrolysate as feedstock is a feasible process even at low pH. The pH fluctuations shaped the microbiome of anaerobic granules and changed the effluent FP profiles. Nevertheless, the granules were able to quickly adapt to the imposed pH fluctuations, restructuring the microbiome composition, and re-establishing the metabolic pathways. Depending on the pH applied, the predominant genera within the biomass varied, which was reflected in the main FP obtained during those periods. The microbiome within the granules was able to adapt in response to the pH applied, highlighting its high plasticity.

The 2D fluorescence spectroscopy captured changes that the applied pH caused on the process performance of the acidogenic reactor, revealing the differences observed in the microbiome and in the FP profiles throughout the operating time. The development of models based on 2D fluorescence for the prediction of FP and SProt concentrations in the reactor effluent showed promising results as good fittings were achieved. Both models were able to capture the tendency of the data even when the accuracy of the prediction was not so high, being mostly useful when applied online to assess these compounds' concentrations continuously. Although in the present work, the fluorescence measurements were performed after sampling, the optical probe can be placed directly inside the reactor and programmed to do fluorescence spectra acquisition at specific times, which will enable us to assess the FP and SProt concentrations in real time during operations without the need for sampling procedures. Therefore, the information captured can be acquired in real-time, quickly, and easily without having any time delay, contributing to better monitoring and control of the process, and if needed, strategies to overcome the disturbances could be quickly applied. The 2D fluorescence can in fact be a very useful and more environmentally friendly tool for regular process monitoring and control, avoiding daily physicochemical analysis, which is time-consuming and leads to waste generation.

ASSOCIATED CONTENT

Supporting Information

The Supporting Information is available free of charge at https://pubs.acs.org/doi/10.1021/acssuschemeng.3c00316.

Feedstock, experimental setup, and individual reactor design; description of the methods for FP, sugar, and microbiological analyses/2D fluorescence; results ob-

https://doi.org/10.1021/acssuschemeng.3c00316
ACS Sustainable Chem. Eng. 2023, 11, 7398−7406

tained for the UASB reactor pseudo-steady-state; detailed results of microbiological analysis; typical fluorescence spectra with the different regions; predicted and experimental FP and SProt concentrations over time (PDF)

AUTHOR INFORMATION

Corresponding Authors

Claudia F. Galinha − *LAQV-REQUIMTE, Chemistry Department, NOVA School of Science and Technology, Universidade NOVA de Lisboa, Caparica 2829-516, Portugal;* orcid.org/0000-0003-0045-2528; Email: cf.galinha@fct.unl.pt

Anouk F. Duque − *Associate Laboratory i4HB - Institute for Health and Bioeconomy, NOVA School of Science and Technology, Universidade NOVA de Lisboa, Caparica 2829-516, Portugal; UCIBIO − Applied Molecular Biosciences Unit, Department of Chemistry, NOVA School of Science and Technology, Universidade NOVA de Lisboa, Caparica 2829-516, Portugal*; Email: af.duque@fct.unl.pt

Authors

Eliana C. Guarda − *Associate Laboratory i4HB - Institute for Health and Bioeconomy, NOVA School of Science and Technology, Universidade NOVA de Lisboa, Caparica 2829-516, Portugal; UCIBIO − Applied Molecular Biosciences Unit, Department of Chemistry, NOVA School of Science and Technology, Universidade NOVA de Lisboa, Caparica 2829-516, Portugal;* orcid.org/0000-0001-9338-328X

Eunice Costa − *CBQF − Centro de Biotecnologia e Química Fina − Laboratório Associado, Escola Superior de Biotecnologia, Universidade Católica Portuguesa, Porto 4169-005, Portugal;* orcid.org/0000-0001-9932-335X

Cátia Gil − *Associate Laboratory i4HB - Institute for Health and Bioeconomy, NOVA School of Science and Technology, Universidade NOVA de Lisboa, Caparica 2829-516, Portugal; UCIBIO − Applied Molecular Biosciences Unit, Department of Chemistry, NOVA School of Science and Technology, Universidade NOVA de Lisboa, Caparica 2829-516, Portugal*

Catarina L. Amorim − *CBQF − Centro de Biotecnologia e Química Fina − Laboratório Associado, Escola Superior de Biotecnologia, Universidade Católica Portuguesa, Porto 4169-005, Portugal;* orcid.org/0000-0002-6756-552X

Paula M. L. Castro − *CBQF − Centro de Biotecnologia e Química Fina − Laboratório Associado, Escola Superior de Biotecnologia, Universidade Católica Portuguesa, Porto 4169-005, Portugal*

Maria A.M. Reis − *Associate Laboratory i4HB - Institute for Health and Bioeconomy, NOVA School of Science and Technology, Universidade NOVA de Lisboa, Caparica 2829-516, Portugal; UCIBIO − Applied Molecular Biosciences Unit, Department of Chemistry, NOVA School of Science and Technology, Universidade NOVA de Lisboa, Caparica 2829-516, Portugal;* orcid.org/0000-0003-4000-1836

Complete contact information is available at: https://pubs.acs.org/10.1021/acssuschemeng.3c00316

Author Contributions

The manuscript was written through contributions of all authors. All authors have given approval to the final version of the manuscript.

Funding

This research was funded by national funds from the FCT—Fundação para a Ciência e a Tecnologia, I.P. through the project PTDC/BTA-BTA/31746/2017, in the scope of projects UIDP/04378/2020 and UIDB/04378/2020 of the Research Unit on Applied Molecular Biosciences—UCIBIO, project LA/P/0140/2020 of the Associate Laboratory Institute for Health and Bioeconomy—i4HB, and the project UIDB/50016/2020 of the Associate Laboratory Centro de Biotecnologia e Química Fina—CBQF. This research was also funded by the Associate Laboratory for Green Chemistry—LAQV, which is financed by national funds from FCT/MCTES (UIDB/50006/2020 and UIDP/50006/2020). E.C.G. gratefully acknowledges FCT for grant SFRH/BD/136300/2018.

Notes

The authors declare no competing financial interest.

ACKNOWLEDGMENTS

The authors acknowledge Super Bock Bebidas S.A. for supplying the anaerobic granules and the brewer's spent grain.

REFERENCES

(1) Carstea, E. M.; Bridgeman, J.; Baker, A.; Reynolds, D. M. Fluorescence Spectroscopy for Wastewater Monitoring: A Review. *Water Res.* **2016**, *95*, 205−219.

(2) Sá, M.; Ramos, A.; Monte, J.; Brazinha, C.; Galinha, C. F.; Crespo, J. G. Development of a Monitoring Tool Based on Fluorescence and Climatic Data for Pigments Profile Estimation in Dunaliella Salina. *J. Appl. Phycol.* **2020**, *32*, 363−373.

(3) Anton, F.; Lindemann, C.; Hitzmann, B.; Reardon, K. F.; Scheper, T. Fluorescence Techniques for Bioprocess Monitoring. *Encycl. Ind. Biotechnol.* **2010**, DOI: 10.1002/9780470054581.eib632.

(4) Marose, S.; Lindemann, C.; Scheper, T. Two-Dimensional Fluorescence Spectroscopy: A New Tool for on-Line Bioprocess Monitoring. *Biotechnol. Prog.* **1998**, *14*, 63−74.

(5) Galinha, C. F.; Carvalho, G.; Portugal, C. A. M.; Guglielmi, G.; Reis, M. A. M.; Crespo, J. G. Two-Dimensional Fluorescence as a Fingerprinting Tool for Monitoring Wastewater Treatment Systems. *J. Chem. Technol. Biotechnol.* **2011**, *86*, 985−992.

(6) Galinha, C. F.; Carvalho, G.; Portugal, C. A. M.; Guglielmi, G.; Reis, M. A. M.; Crespo, J. G. Multivariate Statistically-Based Modelling of a Membrane Bioreactor for Wastewater Treatment Using 2D Fluorescence Monitoring Data. *Water Res.* **2012**, *46*, 3623−3636.

(7) Grote, B.; Zense, T.; Hitzmann, B. 2D-Fluorescence and Multivariate Data Analysis for Monitoring of Sourdough Fermentation Process. *Food Control* **2014**, *38*, 8−18.

(8) Hantelmann, K.; Kollecker, M.; Hüll, D.; Hitzmann, B.; Scheper, T. Two-Dimensional Fluorescence Spectroscopy: A Novel Approach for Controlling Fed-Batch Cultivations. *J. Biotechnol.* **2006**, *121*, 410−417.

(9) Waqas, M.; Rehan, M.; Khan, M. D.; Nizami, A. S. *Conversion of Food Waste to Fermentation Products*; Elsevier, 2019. DOI: 10.1016/B978-0-08-100596-5.22294-4.

(10) Carvalheira, M.; Duque, A. F. Froom Food Waste to Volatile Fatty Acids towards a Circular Economy. *Ferment.-Proc., Benef. Risks* **2021**, 13.

(11) Mussatto, S. I.; Dragone, G.; Roberto, I. C. Brewers' Spent Grain: Generation, Characteristics and Potential Applications. *J. Cereal Sci.* **2006**, *43*, 1−14.

(12) Lynch, K. M.; Steffen, E. J.; Arendt, E. K. Brewers' Spent Grain: A Review with an Emphasis on Food and Health. *J. Inst. Brew.* **2016**, *122*, 553−568.

(13) Kavalopoulos, M.; Stoumpou, V.; Christofi, A.; Mai, S.; Barampouti, E. M.; Moustakas, K.; Malamis, D.; Loizidou, M. Sustainable Valorisation Pathways Mitigating Environmental Pollution from Brewers' Spent Grains. *Environ. Pollut.* **2021**, *270*, No. 116069.

(14) Fărcaş, A.; Tofană, M.; Socaci, S.; Mudura, E.; Scrob, S.; Salanţă, L.; Mureşan, V. Brewers ' Spent Grain − A New Potential Ingredient for Functional Foods. *J Agroaliment Process Technol* **2014**, 137.
(15) Guarda, E. C.; Oliveira, A. C.; Antunes, S.; Freitas, F.; Castro, P. M. L.; Duque, A. F.; Reis, M. A. M. A Two-Stage Process for Conversion of Brewer's Spent Grain into Volatile Fatty Acids through Acidogenic Fermentation. *Appl. Sci.* **2021**, *11*, 3222.
(16) Teixeira, M. R.; Guarda, E. C.; Freitas, E. B.; Galinha, C. F.; Duque, A. F.; Reis, M. A. M. Valorization of Raw Brewers' Spent Grain through the Production of Volatile Fatty Acids. *New Biotechnol.* **2020**, *2020*, 4−10.
(17) Nigam, P. S. An Overview: Recycling of Solid Barley Waste Generated as a by-Product in Distillery and Brewery. *Waste Manage.* **2017**, *62*, 255−261.
(18) APHA; AWWA; WEF *Standard Methods for the Examination of Water and Wastewater*; 21st, Ed.; APHA, American Public Health Association; AWWA, American Water Works Association; WEF, Water Environment Federation: Alexandria, Virginia, USA, 2005.
(19) Duque, A. F.; Oliveira, C. S. S.; Carmo, I. T. D.; Gouveia, A. R.; Pardelha, F.; Ramos, A. M.; Reis, M. A. M. Response of a Three-Stage Process for PHA Production by Mixed Microbial Cultures to Feedstock Shift: Impact on Polymer Composition. *New Biotechnol.* **2014**, *31*, 276−288.
(20) Lowry, O. H.; Rosebrough, N. J.; Farr, A. L.; Randall, R. J. Protein Measurement with the Folin Phenol Reagent. *J. Biol. Chem.* **1951**, *193*, 265−275.
(21) Carvalho, G.; Lemos, P. C.; Oehmen, A.; Reis, M. A. M. Denitrifying Phosphorus Removal: Linking the Process Performance with the Microbial Community Structure. *Water Res.* **2007**, *41*, 4383−4396.
(22) Paulo, A. M. S.; Amorim, C. L.; Costa, J.; Mesquita, D. P.; Ferreira, E. C.; Castro, P. M. L. Long-Term Stability of a Non-Adapted Aerobic Granular Sludge Process Treating Fish Canning Wastewater Associated to EPS Producers in the Core Microbiome. *Sci. Total Environ.* **2021**, *756*, No. 144007.
(23) Bro, R. PARAFAC. Tutorial and Applications. *Chemom. Intell. Lab. Syst.* **1997**, *38*, 149−171.
(24) Andersson, C. A.; Bro, R. The N-Way Toolbox for MATLAB. *Chemom. Intell. Lab. Syst.* **2000**, *52*, 1−4.
(25) Matos, M.; Cruz, R. A. P.; Cardoso, P.; Silva, F.; Freitas, E. B.; Carvalho, G.; Reis, M. A. M. Combined Strategies to Boost Polyhydroxyalkanoate Production from Fruit Waste in a Three-Stage Pilot Plant. *ACS Sustainable Chem. Eng.* **2021**, *9*, 8270−8279.
(26) Gouveia, A. R.; Freitas, E. B.; Galinha, C. F.; Carvalho, G.; Duque, A. F.; Reis, M. A. M. Dynamic Change of PH in Acidogenic Fermentation of Cheese Whey towards Polyhydroxyalkanoates Production: Impact on Performance and Microbial Population. *New Biotechnol.* **2017**, *37*, 108−116.
(27) Itoh, Y.; Tada, K.; Kanno, T.; Horiuchi, J. I. Selective Production of Lactic Acid in Continuous Anaerobic Acidogenesis by Extremely Low PH Operation. *J. Biosci. Bioeng.* **2012**, *114*, 537−539.
(28) Xu, R.; Yang, Z. H.; Zheng, Y.; Liu, J. B.; Xiong, W. P.; Zhang, Y. R.; Lu, Y.; Xue, W. J.; Fan, C. Z. Organic Loading Rate and Hydraulic Retention Time Shape Distinct Ecological Networks of Anaerobic Digestion Related Microbiome. *Bioresour. Technol.* **2018**, *262*, 184−193.
(29) Tahir, K.; Miran, W.; Jang, J.; Shahzad, A.; Moztahida, M.; Kim, B.; Lim, S. R.; Lee, D. S. Carbamazepine Biodegradation and Volatile Fatty Acids Production by Selectively Enriched Sulfate-Reducing Bacteria and Fermentative Acidogenic Bacteria. *J. Chem. Technol. Biotechnol.* **2021**, *96*, 592−602.
(30) Wang, Y.; Wang, C.; Wang, Y.; Xia, Y.; Chen, G.; Zhang, T. Investigation on the Anaerobic Co-Digestion of Food Waste with Sewage Sludge. *Appl. Microbiol. Biotechnol.* **2017**, *101*, 7755−7766.
(31) Feng, K.; Li, H.; Zheng, C. Shifting Product Spectrum by PH Adjustment during Long-Term Continuous Anaerobic Fermentation of Food Waste. *Bioresour. Technol.* **2018**, *270*, 180−188.
(32) Li, B. Y.; Xia, Z. Y.; Gou, M.; Sun, Z. Y.; Huang, Y. L.; Jiao, S. B.; Dai, W. Y.; Tang, Y. Q. Production of Volatile Fatty Acid from Fruit Waste by Anaerobic Digestion at High Organic Loading Rates: Performance and Microbial Community Characteristics. *Bioresour. Technol.* **2022**, *346*, No. 126648.
(33) Carvalho, G.; Pedras, I.; Karst, S. M.; Oliveira, C. S. S.; Duque, A. F.; Nielsen, P. H.; Reis, M. A. M. Functional Redundancy Ensures Performance Robustness in 3-Stage PHA-Producing Mixed Cultures under Variable Feed Operation. *New Biotechnol.* **2018**, *40*, 207−217.
(34) Flaiz, M.; Baur, T.; Brahner, S.; Poehlein, A.; Daniel, R.; Bengelsdorf, F. R. Caproicibacter Fermentans Gen. Nov., Sp. Nov., a New Caproate-Producing Bacterium and Emended Description of the Genus Caproiciproducens. *Int. J. Syst. Evol. Microbiol.* **2020**, *70*, 4269−4279.
(35) Liu, S.; Bischoff, K. M.; Leathers, T. D.; Qureshi, N.; Rich, J. O.; Hughes, S. R. Butyric Acid from Anaerobic Fermentation of Lignocellulosic Biomass Hydrolysates by Clostridium Tyrobutyricum Strain RPT-4213. *Bioresour. Technol.* **2013**, *143*, 322−329.
(36) Zhang, Q.; Lu, Y.; Zhou, X.; Wang, X.; Zhu, J. Effect of Different Vegetable Wastes on the Performance of Volatile Fatty Acids Production by Anaerobic Fermentation. *Sci. Total Environ.* **2020**, *748*, No. 142390.
(37) Lagoa-Costa, B.; Kennes, C.; Veiga, M. C. Cheese Whey Fermentation into Volatile Fatty Acids in an Anaerobic Sequencing Batch Reactor. *Bioresour. Technol.* **2020**, *308*, No. 123226.
(38) Galinha, C. F.; Crespo, J. G. From Black Box to Machine Learning: A Journey through Membrane Process Modelling. *Membranes* **2021**, *11*, 574.

https://doi.org/10.1021/acssuschemeng.3c00316
ACS Sustainable Chem. Eng. 2023, 11, 7398−7406